Optimal LED Placement in Indoor VLC Networks

Anna Maria Vegni[1,*], and Mauro Biagi[2]

[1]*Department of Engineering, Roma Tre University,* 00146 *Rome, Italy.*
[2]*Department of Information, Electrical and Telecommunication (DIET) engineering, "Sapienza" University of Rome,* 00184 *Rome, Italy.*
annamaria.vegni@uniroma3.it

Abstract: In the upcoming 5G systems, the use of optical attocells will be largely exploited, with the aim of extending connectivity to multiple users, while reducing coverage holes in indoor environments. The deployment of light emitting diodes (LEDs) should be well considered in order to use the optimal number of attocells to guarantee both illumination and connectivity, as a large and unnecessary number of attocells in a room is not useful and can cause interference among neighboring lighting cells. On the other hand, a low number of LEDs may not guarantee the whole illumination/data coverage, causing outage to users attempting to access the medium.

In this paper, we investigate the problem of optimal LEDs placement in indoor environments, subject to constraints on illumination and outage based on user data rate. Two approaches are introduced, focusing on (*i*) the minimization of the number of LEDs to be used to provide required services, and (*ii*) the maximization of number of users to be served with a fixed number of LEDs, respectively. Numerical results are carried out in different room scenarios, which distinguish from the probability density function of users laying in such environments.

1. Introduction

Visible Light Communication (VLC) paradigm is expected to be a fundamental technology in the context of 5G networks [1, 2], which are forecasting to incorporate more/smaller cells, additional spectrum, energy efficient communications, mobile convergence, and heterogeneous network integration. Indeed, due to its massive and unlicensed available spectrum, VLC guarantees high data rates, while providing illumination and secure data transmissions. This is therefore a green technology, which can be integrated with existing Radio Frequency (RF) ones, like IEEE 802.11 [3].

In 5G network scenarios, the use of multiple small cells has been proven to improve the network performances, like throughput and spectral efficiency, as well as it provides multi-user connectivity. The use of optical attocells [4] in indoor environments consists that each light-emitting diode (LED) acts as an optical access point (AP) that serves multiple users within its coverage. Furthermore, the use of several attocells is expected to better cover the indoor area, and allows a better resource sharing among users, than a configuration with a limited number of LEDs [5]. However, the deployment of LEDs should be well considered in order to use the optimal number of attocells. Indeed, a large number of attocells in a room is not useful, as it can cause interference among neighbouring lighting cells; as well as a poor number of LEDs suffers to guarantee the whole illumination/data coverage, causing outage to users attempting to access the medium. Moreover, having several attocells may ask to activate handover procedures very frequently so reducing network throughput [5].

In the area of optical networking only a few studies have addressed this issue. Commonly, the design of attocells deployment in indoor environments is based on the grid model, where LED lights are installed in the ceiling with a regular pattern [6, 7]. Usually in an indoor environment the LEDs deployment is done considering fixed and predefined positions, and then the coverage analysis is provided. For instance, Wang *et al.* in [8] investigate the performance of LEDs

deployment to reduce the signal-to-noise ratio fluctuation in a room, as well as Stefan and Haas [9] consider the area spectral efficiency (ASE) as metric to assess the proposed LED deployment. This approach allows assessing the benefits of a given LEDs deployment scheme, but cannot yield which is the best deployment to achieve a given performance. For instance, in a given room, we aim to find the optimal design of LEDs deployment in order to meet illumination and outage probability constraints.

In this paper, we present both a synthesis problem and analysis one. Both are system planning tools to be used off-line before setting up the indoor VLC network. To do so, we propose two approaches for optimal LEDs deployment in indoor environments, aiming to (*i*) minimize the number of attocells to be installed (*synthesis*) in order to meet illumination constraints and a minimum number of users to be served, and (*ii*) maximize the number of users to grant network access (*analysis*), while not exceeding a maximum number of LEDs. The two approaches are similar to each other and assume the existence of an orthogonal access from the LEDs to the users. Of course, as it will be clearly in the next sections, geometry parameters of attocells play an important role to minimize the number of LEDs to be used.

This paper is organized as follows. Section 2 presents an overview of main contributions related to attocells deployments, and we highlight how this paper distinguishes from existing related works. In Section 3 we describe the system model behind this work. Particularly, we analyze how the presence of users in a given room and the room features (*i.e.*, presence of furnitures) can affect the following LED deployment techniques. Section 4 introduces two approaches (*i.e.*, ACM and AUM) to solve the optimal LED deployment under both illumination constraint, and users requirements. In Section 5 numerical results show the effectiveness of the proposed approaches in different room scenarios. Finally, conclusions are drawn at the end of the paper.

2. Related works

The coverage issues of VLC networks have been recently investigated, mainly in the context of hybrid RF and VLC scenarios with mobile users. The need to guarantee communication coverage in hybrid network scenarios is still a challenge [10–12]. Tabassum and Hossain [13] presented a stochastic geometry framework to perform the coverage and rate analysis in co-existing VLC and RF networks. However, when considering only VLC technology, the optimal LEDs placement is still an open issue. How many LEDs need to be deployed is a network design issue, that should be addressed considering both illumination and communications requirements.

In this regard, one performance parameter useful to assess the effectiveness of the LEDs placement in a room is the ASE. In [9], Stefan and Haas investigated the optimum placement of two LED arrays in an indoor VLC scenario, subject to maximization of ASE factor. The authors considered an empty room, without any particular furniture, and aimed at finding optimal solutions of LEDs placement according to different field of view (FOV) values. In [14] the main coverage issues –such as the transmitted power, the dimming factor, and the node failure– have been analyzed in optical domain, considering a network scheme with uniform distribution of LED arrays. In [15] Yin and Haas presented a mathematical framework for the coverage probability analysis in a multi-user VLC scenario, where the LED APs are randomly distributed on the ceiling. Also, the authors distinguished between active and idle APs, assuming for instance underloaded networks with AP sleep strategy to save energy and/or minimize the co-channel interference.

In [16] the authors investigated on three different rectangular LED placement schemes based on geometry features (*i.e.*, presence of voids and overlapping areas). The analysis of coverage aspects has been carried out, taking into account both coverage fraction and interference factor. A similar approach has been presented by the same authors in [17], in case of three hexagonal VLC AP deployment schemes. Finally, in [18] the authors considered multiple transmitters and one receiver, with the enhanced space shift keying modulation. The coverage analysis has been

assessed in such scenario for different values of LEDs characteriscs, and assuming fixed LED positions.

Finally, a different approach to improve the communication coverage in a VLC system has been presented in [19]. The authors did not consider geometric features but assumed a non-Hermitian symmetry orthogonal frequency division multiplexing scheme. Another work from the same authors investigated both illumination and communication coverage issues in a MIMO-VLC system [20].

In all previous works, the VLC APs are deployed in fixed and predefined positions in order to assess the coverage analysis in the whole indoor environment. On the other side, in this paper we aim to identify the possible LEDs deployment schemes that can achieve illumination constraints and multi-user access. In the following subsection, we present the main goals addressed in this paper.

2.1. Goals of the work

The main contributions of this paper can be summarized as follows:

- We define the system model that allows to compute the probability density function (pdf) per user in a given indoor scenario. The pdf depends on the specific environment and the probability that a user will lay in a given position;

- We present two techniques for optimal attocell deployment in indoor scenarios. The first technique, namely AttoCell Minimization (ACM), aims at minimizing the number of attocells that are able to serve a target number of users, with the constraints of outage probability and illumination. Physical parameters of the attocells are taken into account. The second technique, namely Accessing Users Maximization (AUM), aims at evaluating the maximum number of users for an assigned number of LEDs (*i.e.*, attocells), subject to both outage and illumination constraints;

- Numerical results are presented for two indoor scenarios (*i.e.*, an open office room and a museum room) by varying the attocell geometrical parameters (*i.e.*, the half-power semi angle) and requirements (*i.e.*, outage and data rate per user) under the hypothesis of orthogonal access in downlink. ∎

3. System model and network architecture

Let us consider a room whose tridimensional dimensions are d_X, d_Y and d_Z [m], so that the area on the floor is $A = d_X \times d_Y$ m^2. In such a scenario, we can compute the probability density function of a user in the room (*i.e.*, the probability that a user lays in a given position). This is based on the furnishing present in the room (*i.e.*, presence of desks, chairs, closets, and points of interests like coffee machine, blackboard, printer, etc.) and its destination (*i.e.*, house room, university lab, library, etc.). In this way, we can define three different areas related to the probability that a user can stay. This has an impact on the possibility that the network access can be accomplished. The first area, namely *no access area*, is related to all those positions in the room where a user cannot access (*e.g.*, the position of a closet cannot be occupied by the user). In this sense if that area is excluded by the access is not a problem to be solved. Then, the *high-probability area* considers all those positions where we expect the most likely user's access to the network, for example if a table is present, thus meaning that a portable computer can be posed there to work. Last, the *intermediate-probability area*, where the medium access is possible but not so likely as in the high-probability case (*e.g.*, people walking in the room with their smartphone on hand).
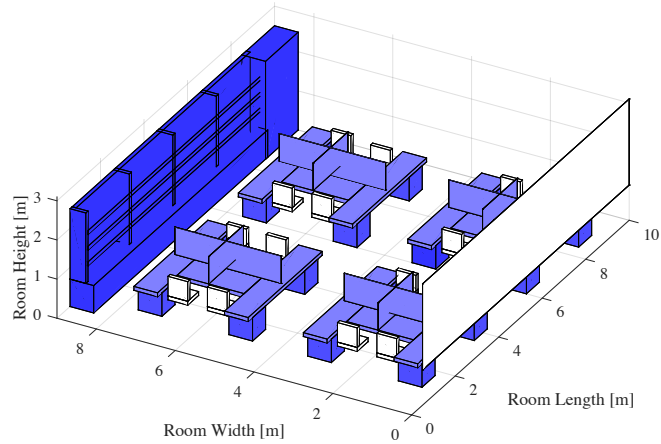
(a)
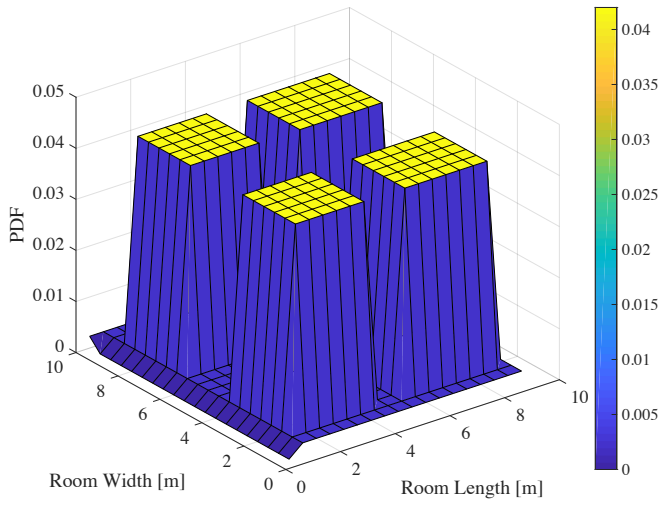
(b)

Fig. 1. Open office scenario. (a) Room configuration, and (b) probability density function.

This allows us to model the presence of a user (and its access request probability) as a bi-variate random variable, characterized by the following step-based functions *i.e.*,

$$p_U(x, y) = p_U^{(1)}(x, y) + p_U^{(2)}(x, y) + p_U^{(3)}(x, y), \tag{1}$$

where $p_U^{(i)}(x, y)$ with $i = \{1, 2, 3\}$ are defined on the bi-dimensional interval $\mathcal{I}_i$ that collects all the positions where access can be requested with medium, high, and null probability, respectively for $i = \{1, 2, 3\}$. It follows that[1] $p_U^{(3)}(x, y) = 0$. Both $p_U^{(1)}(x, y)$ and $p_U^{(2)}(x, y)$ are step-based surfaces that present zero height where the access request cannot be raised, and also, $p_U^{(1)}(x, y)$ presents α height, while $p_U^{(2)}(x, y)$ has β height. Furthermore, in the positions where the access is possible and $p_U^{(1)}(x, y)$ is α, $p_U^{(2)}(x, y)$ will be zero, while in the positions where $p_U^{(1)}(x, y)$ is

---

[1]We use $p_U^{(3)}(x, y)$ just to define $\mathcal{I}_3$ that corresponds to areas where a user cannot lay.
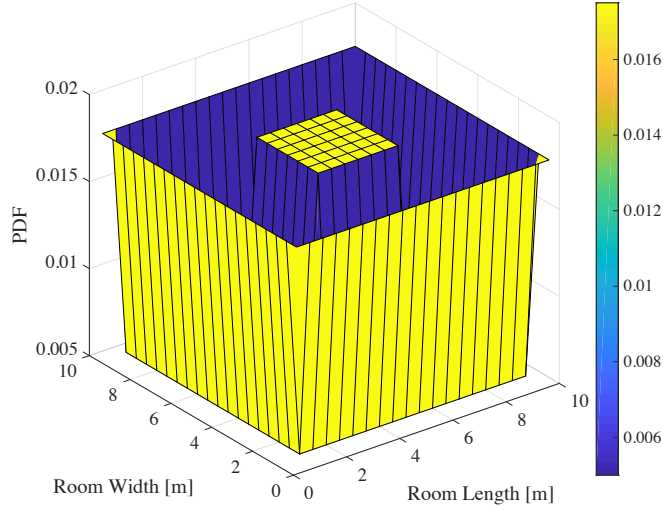
Fig. 2. Probability density function of a museum room configuration.

zero, $p_U^{(2)}(x, y)$ will be β. Analytically, we have that

$$\int \int_{\mathcal{I}_2} p_U^{(2)}(x, y) = P_H, \tag{2}$$

where P_H is the *high probability* of user's access, and we have also that

$$\int \int_{\mathcal{I}_1} p_U^{(1)}(x, y) = 1 - P_H, \tag{3}$$

for the *intermediate probability* P_L, thus meaning that $P_L = 1 - P_H$. As an example, let us consider an open office scenario as depicted in Fig. 1 (a), where we notice the presence of a bookcase, desks and chairs. The corresponding pdf is reported in Fig. 1 (b) under the hypothesis of $P_H = 0.6$ and $P_L = 0.4$. It is possible to note that in correspondence with desks the pdf is high, while it is lower where walking is allowed. Moreover, the pdf is zero in correspondence with the bookcase. It is fundamental to highlight that the analysis carried out in this paper can work with any pdf and, when we consider different environments, we will obtain different LEDs deployment solutions.

Another typical application scenario is a museum room *e.g.*, comprised of a showcase in the middle of the room and several paintings all over the walls. Users are then expected to be in the middle and on the borders of the room with higher probability with respect to the walking area. The associated user pdf is depicted in Fig. 2.

Till now we focused on the position of the single user in the network while, in a more general sense, we need to take into account the joint probability of having the presence of a number of N_U users (*i.e.*, multi-user scenario). When evaluating the average rate due to the presence of N_U users, we need to consider how the multivariate pdf related to positions of the users in the room can be written. As an instance, in case of two uses *i.e.*, U_1 and U_2, the associated joint probability is

$$p_{U_1, U_2}(x_1, y_1, x_2, y_2) = p_{U_2|U_1}(x_2, y_2|x_1, y_1)$$
$$\cdot p_{U_1}(x_1, y_1), \tag{4}$$

where (x_1, y_1) represent the coordinates of U_1, while (x_2, y_2) are related to the coordinates of U_2. Eq. (4) states the impossibility of having two users in the same *tile* by taking into account the probability of U_1 given by $p_{U_1}(x_1, y_1)$, and the position of U_2 conditioned on the position of U_1 *i.e.*, $p_{U_2|U_1}(x_2, y_2|x_1, y_1)$.

Generalizing the analysis to the presence of N_U users, we can describe the joint pdf as in Eq. (5), where each joint probability can be obtained as for Eq. (4) by conditioning with respect to the single variables in order to obtain the *chain* probability *i.e.*,

$$
\begin{aligned}
p_{\mathbf{U}}(\mathbf{x}_{N_U}, \mathbf{y}_{N_U}) = & p_{N_U|U_1, U_2, \ldots, U_{N_U-1}}(x_{N_U}, y_{N_U} | x_{N_1}, y_{N_1}, x_{N_2}, y_{N_2}, \ldots, x_{N_U-1}, y_{N_U-1}) \cdot \\
& \cdot p_{U_1}(x_1, y_1) \cdot p_{U_2}(x_2, y_2) \cdot \ldots \cdot p_{N_U}(x_{N_U}, y_1).
\end{aligned}
\tag{5}
$$

It is worth noting that $\mathbf{U}$ is related to the collection (vector) of all the N_U users variables, while $\mathbf{x}_{N_U}$ and $\mathbf{y}_{N_U}$ are related to the N_U length vectors of coordinates among the x and y directions, respectively.

4. LEDs placement

In this section, we propose two techniques aiming at optimizing the design of the VLC network, considering different goals that are (*i*) the minimization of the number of attocells with the goal of offering the service to an assigned number of users, and (*ii*) the maximization of the number of users to be served once set the number of LEDs to deploy. The two techniques return all the positions of the room where one or more LEDs can be installed, in order to meet all the constraints. Those positions strictly depend on the geometry parameters of the attocells, like the half-power semi angle θ of LEDs, the Lambertian order m, etc., as well as the features of the photodetector, like FOV, the effective physical area, etc.

A user that cannot be served by the LED(s) will experience a data rate lower than a given threshold *i.e.*, the minimum acceptable data rate per user, so leading to an outage. The general expression of the data rate is given by

$$
\mathcal{R} = B \log_2 \left(1 + \frac{P|h|^2}{\mathcal{N}_0 B \Gamma} \right),
\tag{6}
$$

where B [Hz] is the available bandwidth, P [W] is the transmitted power, h is the DC channel response, $\mathcal{N}_0$ [W] is the noise power, and Γ takes into account for the Signal-to-Noise Ratio (SNR)-gap required to achieve error rate performance as in [21]. It is important to highlight that the channel coefficient depends both on the position of the LED and also of the receiving user. This means that, by considering the k-th coordinates of the k-th user as (x_k, y_k), when we fix the ℓ-th LED coordinates (x_ℓ, y_ℓ), we have that the rate can be rewritten as

$$
\mathcal{R}(x_\ell, y_\ell, x_k, y_k) = B \log_2 \left(1 + \frac{P|h(x_\ell, y_\ell, x_k, y_k)|^2}{\mathcal{N}_0 B \Gamma} \right).
\tag{7}
$$

Hence, we can write the average rate conditioned on the position of the ℓ-th LED as

$$
\overline{\mathcal{R}}(x_\ell, y_\ell) = \int \int_{\mathcal{I}_U} \mathcal{R}(x_\ell, y_\ell, x_k, y_k) p_U(x_k, y_k) dx_k dy_k,
\tag{8}
$$

and this works for the single user in the network with reference to the generic LED position and $\mathcal{I}_U$ gathers the areas in the room related to high, medium and zero probability as reported before in Eq.(1).

From the definition of the data rate per user, we can derive the outage probability, expressed in terms of average rate per user *i.e.*, $\overline{\mathcal{R}}$. We recall that the outage event occurs when the rate per

user cannot be achieved. The average rate over the room, conditioned to the position of the LEDs, is given by

$$\overline{\mathcal{R}}\left(\mathbf{x}_{N_U}, \mathbf{y}_{N_U} \mid \mathbf{x}_L, \mathbf{y}_L\right) =$$

$$= \sum_{\ell=1}^{L} \int \int \mathcal{R}\left(x_\ell, y_\ell, \mathbf{x}_U, \mathbf{y}_U\right) \cdot \tag{9}$$

$$\cdot p_{\mathbf{U}}\left(\mathbf{x}_{N_U}, \mathbf{y}_{N_U}\right) d\mathbf{x}_{N_U} d\mathbf{y}_{N_U},$$

where the integration is operated on the multivariate distribution introduced in Eq. (5) that takes into account the presence of all the users in the network. The vectors $\mathbf{x}_L, \mathbf{y}_L$ take accounts for the positions of the L LEDs in the network. The summation over ℓ considers the possibility of granting access to users also by multiple overlapping LEDs light still under the hypothesis of orthogonal access within attocells and among attocells. This allows to define the outage as the probability of being unable to guarantee a target average rate per user $\mathcal{R}^\star$, *i.e.*,

$$P_{out} = \Pr\{\overline{\mathcal{R}}(\mathbf{x}_{N_U}, \mathbf{y}_{N_U} \mid \mathbf{x}_L, \mathbf{y}_L) \leq \mathcal{R}^\star)\}. \tag{10}$$

Hence, once defined the position of LEDs, it is possible to evaluate the outage with respect to the probability of users positions. For sake of simplicity and allowing a simple numerical computation, it is possible to operate a spatial sampling of the room so as to have $N_x N_y$ square tiles each one of $a = A/(N_x N_y)$ dimension and this allows to simplify all integrations since they become sums.

4.1. AttoCells Minimization and LEDs placement

The problem of optimal LEDs deployment can be addressed according to the following considerations [5]. Having too few attocells (as limit, only one) leads to share the resource among users so leading to data rate reduction. On the other hand, organizing the network coverage by resorting to the use of several attocells can induce severe delays due to numerous handovers to be performed by users even in the case of limited mobility as for a VLC network.

Hence, we try to solve the following problem:

$$\begin{aligned} & \min N_C \\ & s.t. \ \ P_{out} \leqslant \delta \\ & \quad\quad I \geqslant I_{\min} \\ & \quad\quad N_U = U_{\min} \end{aligned} \tag{11}$$

that is the minimization of the number of attocells N_C, subject to (*i*) the outage probability P_{out} is at least equal to or lower than a given threshold δ, (*ii*) the illumination level I is at least equal to or higher than the minimum intensity level $I_{\min}$ for the illumination in all the room, and (*iii*) the number of users N_U to be served is the minimum $U_{\min}$. The technique that fixes this problem is then named AttoCells Minimization (ACM).

The solution of the problem in Eq. (11) can be found by resorting to the exhaustive search with respect to the position of the LED(s). We remind that this kind of optimization needs to be performed offline, before the setup of the network. Even though at a first glance the method can appear costly, as will be clear in the following, this procedure does not result to be heavy. It is important to highlight that when the network constraints are assigned in terms of number of users to be served, rate per user, and other physical layer parameters, the solution of the above problem gives both the number and the positions of the LEDs to provide network access. We discuss the feasibility of the problem at the end of the numerical results.

The optimization procedure will follow an iterative approach that is, an implementation of the exhaustive search as follows. At first, given the minimum illumination constraint to be satisfied

all over the room despite of pdf, for the desired number of users $U_{\min}$, initially the solution with $N_C = 1$ will be explored. All the possible single LED placements in the room will be checked, and the outage probability in Eq. (10) will be computed. Just in case that all the constraints in Eq. (11) are met, $N_C = 1$ and the LED position granting the satisfaction of all the requirements is the solution of the problem. If no LED positions are able to satisfy all the constraints, $N_C = 2$ will be considered as possible solution by considering LEDs placement pairs in the room and, as for the previous case, checking if all the constraints are satisfied. This iteration continues till achieving the solution of the problem, *i.e.*, the minimum number of LEDs that satisfy all the constraints and their positions.

4.2. Accessing User Maximization and LEDs placement

The second problem we tackle is the optimal LEDs placement in the room, by considering as constraints (*i*) the illumination level, (*ii*) the number of LEDs to be used, and (*iii*) the outage probability. We try to find the optimal LEDs deployment so as to maximize the number of users to be served by the network. Even though slightly different from the previous problem, this allows to understand how many users can be *covered* with a given LEDs configuration and this can be of important impact when a hybrid access (VLC/RF) is taken into account. Specifically, we can formalize the problem as follows:

$$
\begin{aligned}
\max\ & N_U \\
s.t.\ & P_{out} \leqslant \delta \\
& N_C = N_C^{\max} \\
& I \geq I_{\min}
\end{aligned}
\tag{12}
$$

that represents the maximization of the number of users to be served (*i.e.*, N_U) subject to (*i*) the outage probability P_{out} is at least equal to or lower than the threshold δ, (*ii*) the number of LEDs is the maximum allowed (*i.e.*, $N_C^{\max}$), and (*iii*) the illumination level I is at least equal to or higher than the minimum level (*i.e.*, $I_{\min}$).

Analogously to the ACM technique, the solution to the problem can be pursued by considering exhaustive search with respect to the position of the LEDs. In this regard, by assuming that the number of cells is given by $N_C^{\max}$, we explore all the possible placements for LEDs in the room, at the beginning for $N_U = 1$. The same procedure is then iterated for $N_U = 2$, and so forth. The maximum number $N_U^\star$ that is the last able to satisfy all the constraints (thus meaning that $N_U^\star + 1$ is not allowed), will be the solution of the problem, jointly with the LEDs placement allowing the achievement of all the constraints.

This technique aiming at maximizing the number of users to be served, subject to illumination, outage and attocells constraints, is then named as Accessing User Maximization (AUM).

5. Numerical results

In this section we provide numerical results of the two techniques ACM and AUM, expressed in terms of (*i*) minimum number of attocells that satisfies the solution in Eq. (11), and (*ii*) the maximum number of users that can be served according to the constraints in Eq. (12), respectively.

Numerical results have been carried out in two different room scenarios *i.e.*, an open office and a museum room, whose pdfs are depicted in Fig. 1 and Fig. 2, respectively. We assume that each LED presents a transmission bandwidth of 10 MHz, and the power emitted by each white LED is 10 W. It is important to underline that when the coverage areas overlap we assume that it is possible to merge the two channels if it is worth to achieve the minimum required rate, so avoiding outage. If not differently specified, the illumination constraint on the 90 m^2 room is set to 11.1 Lux on the floor corresponding to a flux of 1000 lumen. Furthermore, other parameters are the Lambertian order $m = 2$, the photodiode area set to 0.25 cm^2, and FOV = 60°. We
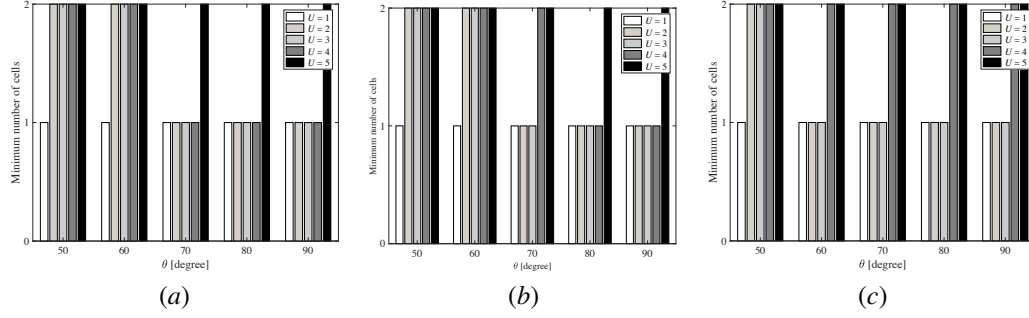
Fig. 3. ACM in open office scenario, in case of (a) $\mathcal{R} = 10$ Mb/s, (b) $\mathcal{R} = 25$ Mb/s, and (c) $\mathcal{R} = 50$ Mb/s.
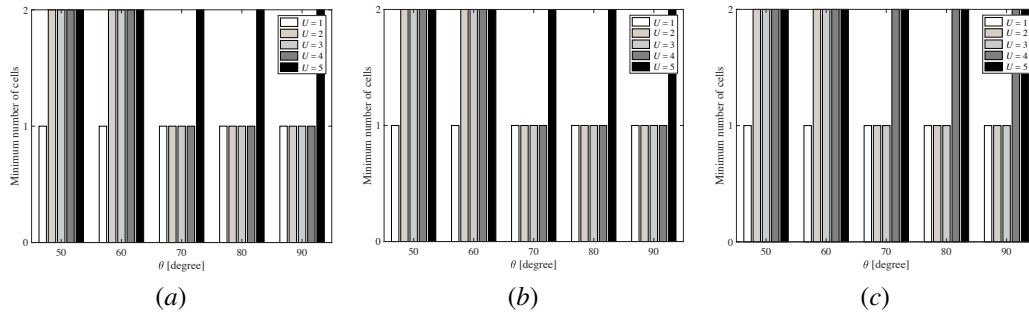

Fig. 4. ACM in museum room scenario, in case of (a) $\mathcal{R} = 10$ Mb/s, (b) $\mathcal{R} = 25$ Mb/s, and (c) $\mathcal{R} = 50$ Mb/s.

highlight that when a certain number of users are declared as *covered* with a solution represented by the number of LEDs, this implies that exists at least one LED(s) placement able to guarantee the performance with the target outage that is set to 1%. In both two scenarios, we consider the case of a data rate per user equal to (*i*) 10 Mb/s, (*ii*) 25 Mb/s, and (*iii*) 50 Mb/s.

5.1. Angle and coverage dependency

In the open office scenario, we compute the minimum number of attocells that can satisfy user requirements subject to illumination constraints. Fig. 3 (a) and (b) depict the solutions of Eq. (11) for different values of θ *i.e.*, $\theta = \{50, 60, 70, 80, 90\}$ degrees, by varying the minimum number of users that are served with a data rate per user of $\mathcal{R} = 10$ Mb/s, $\mathcal{R} = 25$ Mb/s and $\mathcal{R} = 50$ Mb/s, respectively. As θ increases, the minimum number of LEDs that can guarantee the target rate per user decreases, thus meaning that the size of a single attocell is increasing too and the data coverage is guaranteed over more positions in the room. As an instance, as shown in Fig. 3 (a), for $\theta = 90°$ there is at least one cell that can guarantee coverage up to 4 users, while 2 cells are necessary to serve at least 5 users, with a minimum data rate per user of 10 Mb/s. When the half-power semiangle θ decreases, a single LED can guarantee coverage to one user only in case of $\theta = 50°$.

In Fig. 3 (b), when the data rate per user increases *i.e.*, $\mathcal{R} = 25$ Mb/s, the minimum number of cells guaranteeing user requirements increases, as expected. For instance, for $\theta = 70°$, two cells are necessary to cover all the possible positions of at least three users in the open office; for the same conditions –but a lower data rate per user– the minimum number of cells is one, which
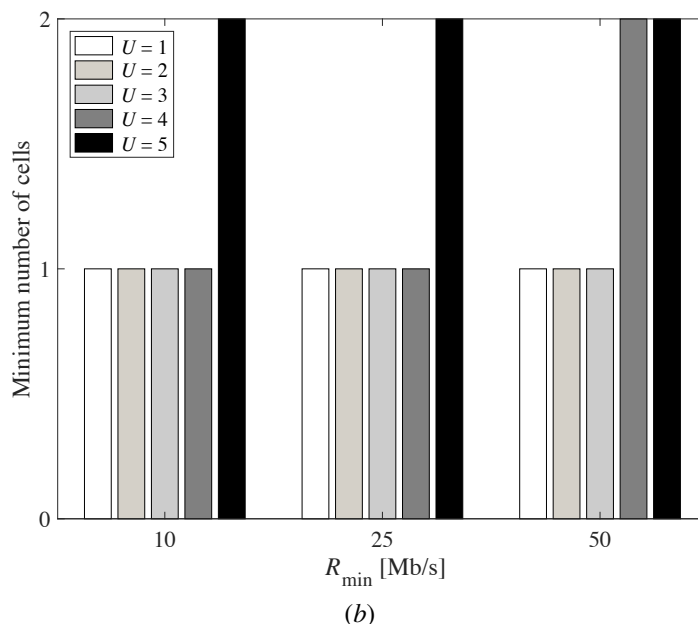
Fig. 5. ACM in open office, for $\theta = 70°$.

becomes two for $\theta = 60°$, as shown in Fig. 3 (a). In case of higher data rate per user –see Fig. 3 (c)– we observe an increasing number of cells that can satisfy such requirements. As a matter, two cells are needed to serve four users at $\mathcal{R} = 50$ Mb/s each, for $\theta = 90°$, while only one cell is a solution of the system for $\theta = 90°$ (see in Fig. 3 (a)), guaranteeing coverage up to four users.

In Fig. 4 (a), similar considerations apply in case of the museum scenario for $\mathcal{R} = 10$ Mb/s, but we observe the problem of minimizing the number of cells is solved with two cells for low half-power semiangles (*i.e.*, $\theta = [50, 60]$ degree), in case of multiple users (*i.e.*, $U_{min} \geq 2$). For increasing θ, there is a minimum number of users that can be satisfied by a single cell (*i.e.*, up to four users with a single cell, for $\theta = 90°$). Similar considerations exist for increasing data rate per users, as depicted in Fig. 4 (c), where at least two cells are needed to satisfy four users even in case of higher half-power semiangle (*i.e.*, $\theta = 90°$).

For comparison purpose, we observe that in case of open office scenario, the system requires more cells (*i.e.*, two cells) to guarantee service to at least three users for $\mathcal{R}_{min} = 25$ Mb/s, and four users for $\mathcal{R}_{min} = 50$ Mb/s. On the other side, in the museum room scenario, the solution is guaranteed by one attocell up to four users up to 25 Mb/s, while 50 Mb/s is provided by two attocells for at least four users.

Finally, we investigate how much the minimum rate requested by the users affects the proposed ACM approach. Fig. 5 depicts the minimum number of cells that guarantee coverage in the museum scenario, to different users requiring variable data rate (*i.e.*, $\mathcal{R}_{min} = [10, 25, 50]$ Mb/s), for a given half power semi-angle (*i.e.*, $\theta = 70°$). For increasing user rate, the minimum number of LEDs (*i.e.*, attocells) increases too.

Moving now to discuss the results affordable by considering the AUM, we observe that in Fig. 6 when the half-power semiangle is low, the coverage offered by a single attocell is low in terms of area and, more, the possible users that can achieve the target rate is low. In fact, having low angles means reducing coverage and so excluding users from the access at the target rate. By increasing the angle, the number of users that can be covered increases too. Also, when a increasing number
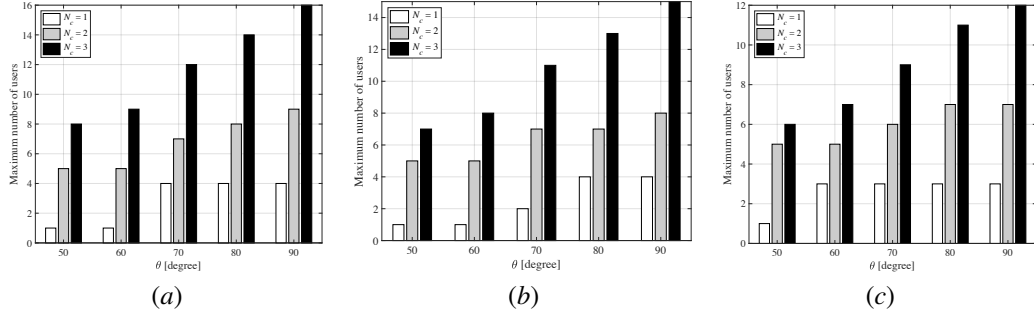
Fig. 6. AUM in open office scenario, in case of (a) $\mathcal{R}$ = 10 Mb/s, (b) $\mathcal{R}$ = 25 Mb/s, and (c) $\mathcal{R}$ = 50 Mb/s.

of attocells is considered, the opportunity of having overlapping areas allow to serve more users with the target rate. It is possible to infer that, for example, in Fig. 6 (a), the number of users served by a single attocell, when the target rate is 10 Mb/s ranges from 1 (*i.e.*, for θ = 50°) to 4 (*i.e.*, for θ = 90°). On the other hand, when the number of attocells grows till to 3, then from 6 to 12 users can be served at target rate.

A similar behavior can be observed in Fig. 6 (b) for a target rate of 25 Mb/s. With respect to the previous case in Fig. 6 (a), here the number of users served for the same number of attocells is lower due to the higher request in terms of rate. Hence, while for 10 Mb/s two attocells can give access up to 9 users for θ = 90° as shown in Fig. 6 (a), here that number reduces to 8. As a consequence, similar considerations apply when a rate of 50 Mb/s per user is considered, as depicted in Fig. 6 (c), where for 3 attocells at θ = 90° we are able to provide access to 12 users, while for the case of 10 Mb/s and 25 Mb/s that number is 16 and 15, respectively.

An analogous situation is met when we consider the museum topology. Still, we report in Fig. 7 (a), (b), and (c) the maximum number of users that can access the network for a predetermined number of attocells for different angles and at target rate of 10 Mb/s, 25 Mb/s, and 50 Mb/s, respectively. Once more, increasing the angle allows to have broader area covered and, when multiple attocells are considered, the overlapping areas may increase so giving the opportunity of taking the access from one or the neighboring attocells *i.e.*, using multiple channels. In this regard, in Fig. 7 (a) by increasing the half-power angle for a single attocell we can grant the access to a number of users ranging from 1 to 4. If we consider the behavior of the system when the target rate is 25 Mb/s as in Fig. 7 (b), a direct comparison with the case reported in Fig. 7 (a) gives evidence of the reduction of the number of users served *i.e.*, 4, 10 and 16 users at 25 Mb/s, and 4, 11 and 17 users at 10 Mb/s, for θ = 90° and N_C = {1, 2, 3} attocells in Fig. 7 (b) and Fig. 7 (a), respectively. A similar behavior is exhibited in case of a target rate of 50 Mb/s as the number of users served is 3, 9 and 14, for θ = 90° and N_C = {1, 2, 3}, respectively.

5.2. Outage dependency

Additionally, in order to consider the effect of outage on the ACM technique, we report in Fig. 8 the minimum number of attocells requested as a function of the outage that the network can sustain in case of multi-user scenario for a target rate of 50 Mb/s, in the museum room configuration. The outage level δ ranges from 0.03% to 3%.

It is possible to appreciate that when the outage increases the number of requested attocells is lower as the system fails to meet the data rate or illumination constraints in several areas of the room. So, for U = 3 we need 2 attocells when δ = 0.3%, while with the number of users raising to 5 we need 3 attocells. Only 1 attocell is necessary when δ = 3% both for single and multiple
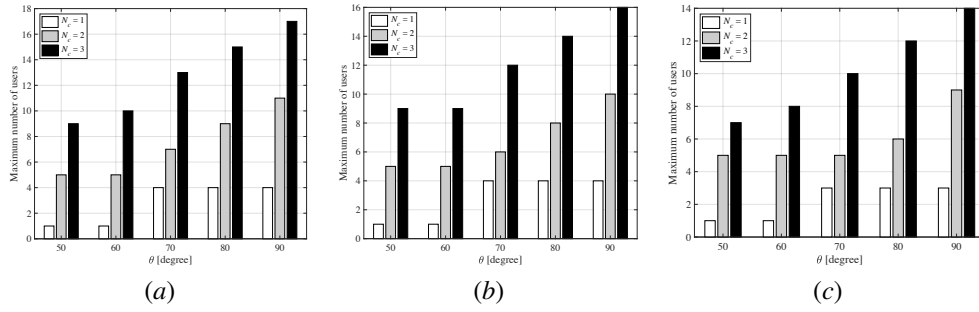
Fig. 7. AUM in museum scenario, in case of (a) $\mathcal{R} = 10$ Mb/s, (b) $\mathcal{R} = 25$ Mb/s, and (c) $\mathcal{R} = 50$ Mb/s.
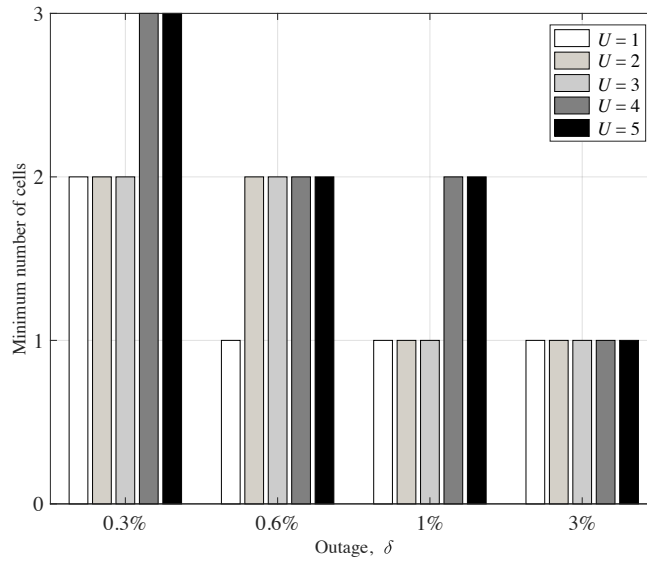

Fig. 8. ACM in museum room scenario vs. outage, for $\mathcal{R}_{min} = 50$ Mb/s.

users. Basically, for increasing outage the minimum number of attocells decreases, as well as for increasing users the minimum number of attocells increases.

A similar performance metric is reported in Fig. 9, by considering the maximum number of users served with an assigned number of attocells, still in case of outage level ranging from 0.03% to 3%, and in the museum room scenario. In this case the number of users increases by increasing the maximum allowed outage. This is due to the possibility of serving users less reliably and, so, the access is granted to higher number of users since their access is not guaranteed in almost all the positions of the room. As an instance, with 2 attocells we serve 9 users when $\delta = 0.03\%$, while when the number of attocells achieves 3 the number of served users ranges from 5 to 11 for $\delta = [0.3\%, 3\%]$, respectively. Similar considerations apply in case of open office room scenario.

5.3. LED placement and solutions

Before concluding, it is important to give evidence of the feasibility of solutions, that is, LEDs placement. Till now, we report the number of attocells needed without showing LEDs positions
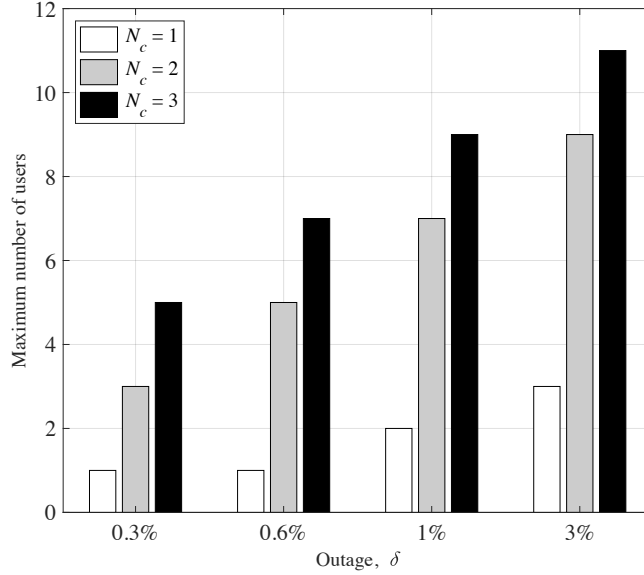
Fig. 9. AUM in museum room scenario vs. outage, for $\mathcal{R}_{\min} = 50$ Mb/s.

Table 1. Percentage of solutions for different values of $\mathcal{R}$ and N_C when $\theta = 70°$, $U = 4$, step for LED placement set to 0.5 meters.

	$\mathcal{R} = 10$ Mb/s	$\mathcal{R} = 40$ Mb/s	$\mathcal{R} = 70$ Mb/s
$N_C{=}1$	95%	1%	0%
$N_C{=}2$	100%	22%	8%
$N_C{=}3$	100%	46%	19%

in the considered scenarios. A clear visualization is not trivial since, sometimes, several positions for a single attocell (*i.e.*, $N_C = 1$) allow to achieve the constraints. More complicated to show is the case for $N_C \geq 2$, as showing pair (or triplets and so forth) of positions over a map is not of easy understanding. Hence, in order to provide a view about how much strict is a solution (only few positions allowing to meet constraints or a lot), we report in Table 1 how many positions are solutions of Eq. (11), and that allow the achievement of all constraints, in case of the museum room scenario with $\theta = 70°$, $U = 4$, and step for attocell placement set to 0.5 meters. Notice that –as expected– for increasing data rate per single user the number of solutions decreases, while it increases for a fixed data rate and increasing attocells.

This means that there are fewer places on the ceiling where the attocell(s) can be posed in order to meet all the constraints. In particular, when a single attocell is used with the data rate constraint of 10 Mb/s per user, we are able to provide access up to 95% of all the positions in the room, while the remaining 5% does not guarantee access (*e.g.*, if the attocell is deployed at the corners of the room). On the other hand if the required rate per single user is 70 Mb/s, no solution exists (*i.e.*, 0%). This does not mean that the problem is not feasible since it exists a higher number of LEDs leading to the solution. In this sense the problem is always feasible. Hence, the problem is solved by deploying 2 attocells in the room, since when the data rate is low (*i.e.*, 10 Mb/s), independently of LEDs position we can grant access to all the users (*i.e.*, 100%).

For the case of 70 Mb/s, we have that only 8% of positions allows the access with 2 attocells. Last, when 3 attocells providing 70 Mb/s per single user are deployed, up the 19% of positions leads to meet all the constraints.

6. Conclusions

In this paper, we proposed two techniques (*i.e.*, ACM and AUM) for optimal attocells deployment in indoor environments, in order to address user requirements and illumination constraints. ACM aims to minimize the number of attocells that can serve a given number of users, subject to outage probability and illumination constraints, while AUM maximizes the number of users that can be served by a predetermined number of attocells. Numerical results show that –as expected– better performance (*i.e.*, low number of attocells and high number of users in case of ACM and AUM, respectively) can be guaranteed in case of large half-power semiangle, and lower data rate per user requirement.

It has been observed that one attocell can guarantee service up to four users with a large half-power semiangle (*i.e.*, $\theta = 90°$). When increasing the data rate per user, a lower number of solutions can be obtained (*e.g.*, 12 users at $\mathcal{R} = 50$ Mb/s can be served by 3 attocells for $\theta = 90°$, while up to 16 users in case of $\mathcal{R} = 10$ Mb/s).

References and links

1. M. B. Rahaim and T. D. C. Little, "Toward practical integration of dual-use VLC within 5G networks," in *IEEE Wireless Communications*, vol. 22, no. 4, pp. 97-103, August 2015. doi: 10.1109/MWC.2015.7224733
2. L. Feng, R. Q. Hu, J. Wang, P. Xu and Y. Qian, "Applying VLC in 5G Networks: Architectures and Key Technologies," in IEEE Network, vol. 30, no. 6, pp. 77-83, November-December 2016. doi: 10.1109/MNET.2016.1500236RP
3. M. Ismail, M. Zeeshan Shakir, K. A. Qaraqe and E. Serpedin, "Radio Frequency and Visible Light Communication Internetworking," in Green Heterogeneous Wireless Networks, IEEE, 2016.
4. H. Haas, "High-speed wireless networking using visible light," SPIE Newsroom, vol. 1, pp. 1-3, Apr. 2013.
5. S. Pergoloni, M. Biagi, S. Colonnese, R. Cusani and G. Scarano, "Optimized LEDs Footprinting for Indoor Visible Light Communication Networks", *IEEE Photonics Technology Letters*, vol. 28, no. 4, pp. 532-535, Feb.15, 15 2016.
6. T. Komine and M. Nakagawa, "Fundamental analysis for visible- light communication system using LED lights," in IEEE Transaction on Consumer Electronics, vol. 50, no. 1, pp. 100-107, Feb. 2004.
7. C. Chen, D. A. Basnayaka, and H. Haas, "Downlink performance of optical attocell networks," in Journal of Lightweight Technology, vol. 34, no. 1, pp. 137-156, Jan. 1, 2016.
8. Z. Wang, C. Yu, W.-D Zhong, J. Chen, and W. Chen, "Performance of a novel LED lamp arrangement to reduce SNR fluctuation for multi-user visible light communication systems," in Optics Express, vol. 20, pp. 4564-4573, 2012.
9. I. Stefan and H. Haas, "Analysis of Optimal Placement of LED Arrays for Visible Light Communication," in *Proc. of IEEE 77th Vehicular Technology Conference (VTC Spring)*, Dresden, 2013, pp. 1-5. doi: 10.1109/VTC-Spring.2013.6691890
10. H. Chowdhury and M. Katz, "Data Download on Move in Indoor Hybrid (Radio-Optical) WLAN-VLC Hotspot Coverages," in *Proc. of IEEE 77th Vehicular Technology Conference (VTC Spring)*, Dresden, 2013, pp. 1-5. doi: 10.1109/VTCSpring.2013.6692499
11. M. R. Zenaidi, Z. Rezki, M. Abdallah, K. A. Qaraqe and M. S. Alouini, "Achievable Rate-Region of VLC/RF Communications with an Energy Harvesting Relay," in *Proc. of GLOBECOM 2017 - 2017 IEEE Global Communications Conference*, Singapore, 2017, pp. 1-7. doi: 10.1109/GLOCOM.2017.8254192
12. X. Bao, X. Zhu, T. Song and Y. Ou, "Protocol Design and Capacity Analysis in Hybrid Network of Visible Light Communication and OFDMA Systems," in *IEEE Transactions on Vehicular Technology*, vol. 63, no. 4, pp. 1770-1778, May 2014. doi: 10.1109/TVT.2013.2286264
13. H. Tabassum and E. Hossain, "Coverage and Rate Analysis for Co-Existing RF/VLC Downlink Cellular Networks," in *IEEE Transactions on Wireless Communications*, vol. 17, no. 4, pp. 2588-2601, April 2018. doi: 10.1109/TWC.2018.2799204
14. A. Vavoulas, H. G. Sandalidis, T. A. Tsiftsis and N. Vaiopoulos, "Coverage Aspects of Indoor VLC Networks," in *Journal of Lightwave Technology*, vol. 33, no. 23, pp. 4915-4921, Dec.1, 1 2015. doi: 10.1109/JLT.2015.2492420
15. L. Yin and H. Haas, "Coverage Analysis of Multiuser Visible Light Communication Networks," in *IEEE Transactions on Wireless Communications*, vol. 17, no. 3, pp. 1630-1643, March 2018. doi: 10.1109/TWC.2017.2782694
16. Shashikant, R. Saini and A. Gupta, "Comparative analysis of coverage aspects for various LEDs placement schemes in indoor vlc system," in *Proc. of 2nd International Conference for Convergence in Technology (I2CT)*, Mumbai, 2017, pp. 487-491. doi: 10.1109/I2CT.2017.8226177

17. Shashikant, P. Garg and A. Gupta, "Comparative analysis of hexagonal VLC nodes deployment schemes," in *Proc. of 4th International Conference on Signal Processing, Computing and Control (ISPCC)*, Solan, 2017, pp. 368-372. doi: 10.1109/ISPCC.2017.8269705

18. S. Menounou, A. N. Stassinakis, H. E. Nistazakis, G. S. Tombras and H. G. Sandalidis, "Coverage area estimation for high performance eSSK visible light communication systems," in *Proc. of Panhellenic Conference on Electronics and Telecommunications (PACET)*, Xanthi, 2017, pp. 1-4. doi: 10.1109/PACET.2017.8259983

19. C. Chen, W. D. Zhong and Dehao Wu, "Communication coverage improvement of indoor SDM-VLC system using NHS-OFDM with a modified imaging receiver," in *Proc. of IEEE International Conference on Communications Workshops (ICC)*, Kuala Lumpur, 2016, pp. 315-320. doi: 10.1109/ICCW.2016.7503806

20. C. Chen, W. D. Zhong and D. Wu, "On the coverage of multiple-input multiple-output visible light communications [Invited]," in *IEEE/OSA Journal of Optical Communications and Networking*, vol. 9, no. 9, pp. D31-D41, Sept. 2017. doi: 10.1364/JOCN.9.000D31

21. A. Garcia-Armada, "SNR gap approximation for M-PSK-Based bit loading", *IEEE Transactions on Wireless Communications*, vol. 5, no. 1, pp. 57-60, Jan. 2006.